

# Noninvasive pressure difference mapping derived from 4D flow MRI in patients with unrepaired and repaired aortic coarctation

Fabian Rengier<sup>1,2</sup>, Michael Delles<sup>3</sup>, Joachim Eichhorn<sup>4</sup>, Yoo-Jin Azad<sup>3</sup>, Hendrik von Tengg-Kobligk<sup>1,5</sup>, Julia Ley-Zaporozhan<sup>1</sup>, Rüdiger Dillmann<sup>3</sup>, Hans-Ulrich Kauczor<sup>1</sup>, Roland Unterhinninghofen<sup>3</sup>, Sebastian Ley<sup>1</sup>

<sup>1</sup>University Hospital Heidelberg, Department of Diagnostic and Interventional Radiology, Im Neuenheimer Feld 110, 69120 Heidelberg, Germany;

<sup>2</sup>German Cancer Research Center (dkfz) Heidelberg, Department of Radiology, Im Neuenheimer Feld 280, 69120 Heidelberg, Germany; <sup>3</sup>Karlsruhe Institute of Technology (KIT), Department of Informatics, Institute for Anthropomatics and Robotics, Adenauerring 2, 76131 Karlsruhe, Germany;

<sup>4</sup>University Hospital Heidelberg, Department of Paediatric Cardiology, Im Neuenheimer Feld 430, 69120 Heidelberg, Germany; <sup>5</sup>Inselspital, University Hospital Bern, Institute for Diagnostic, Interventional and Pediatric Radiology (DIPR), Freiburgstr. 10, 3010 Bern, Switzerland

Correspondence to: Fabian Rengier, MD. University Hospital Heidelberg, Department of Diagnostic and Interventional Radiology, Im Neuenheimer Feld 110, 69120 Heidelberg, Germany. Email: fabian.rengier@web.de.

**Purpose:** To develop a method for computing and visualizing pressure differences derived from time-resolved velocity-encoded three-dimensional phase-contrast magnetic resonance imaging (4D flow MRI) and to compare pressure difference maps of patients with unrepaired and repaired aortic coarctation to young healthy volunteers.

**Methods:** 4D flow MRI data of four patients with aortic coarctation either before or after repair (mean age 17 years, age range 3-28, one female, three males) and four young healthy volunteers without history of cardiovascular disease (mean age 24 years, age range 20-27, one female, three males) was acquired using a 1.5-T clinical MR scanner. Image analysis was performed with in-house developed image processing software. Relative pressures were computed based on the Navier-Stokes equation.

**Results:** A standardized method for intuitive visualization of pressure difference maps was developed and successfully applied to all included patients and volunteers. Young healthy volunteers exhibited smooth and regular distribution of relative pressures in the thoracic aorta at mid systole with very similar distribution in all analyzed volunteers. Patients demonstrated disturbed pressures compared to volunteers. Changes included a pressure drop at the aortic isthmus in all patients, increased relative pressures in the aortic arch in patients with residual narrowing after repair, and increased relative pressures in the descending aorta in a patient after patch aortoplasty.

**Conclusions:** Pressure difference maps derived from 4D flow MRI can depict alterations of spatial pressure distribution in patients with repaired and unrepaired aortic coarctation. The technique might allow identifying pathophysiological conditions underlying complications after aortic coarctation repair.

**Keywords:** Aorta; aortic coarctation; pressure difference mapping; magnetic resonance imaging (MRI); three-dimensional imaging

Submitted Sep 16, 2013. Accepted for publication Dec 03, 2013.

doi: 10.3978/j.issn.2223-3652.2014.03.03

View this article at: <http://www.thecdt.org/article/view/3638/4518>

## Introduction

Aortic coarctation accounts for about 5-7% of all congenital cardiovascular diseases. Hemodynamically significant coarctation is usually treated by surgical or endovascular repair which greatly reduce morbidity (1,2). However, complications can occur at any time after repair and thus

necessitate regular follow-up. Complications include arterial hypertension, recurrent coarctation, aneurysm formation and premature atherosclerosis.

Only few previous studies described factors associated with the occurrence of complications after aortic coarctation repair. For example, age at surgery, coexistence of bicuspid

aortic valve, residual pressure gradient, hypoplastic aortic arch and patient size are related to recurrence of coarctation or aneurysm formation (3,4). Generally, complications are considered to be of multifactorial origin. Altered vascular geometry and disturbed hemodynamics have been discussed as mediating or even underlying factors in the development of complications (4-6).

The pressure gradient across the stenosis is the most important hemodynamic parameter for clinical management of aortic coarctation before and after repair. Currently, pressure gradients are either measured by invasive catheterization, estimated by echocardiography using the Bernoulli equation or approximated by the arm-leg pressure difference. All these methods have relevant limitations. First, the gold standard catheterization requires radiation and is an invasive procedure with its inherent risks. Second, pressure estimations by echocardiography are operator dependent and very sensitive to measurement errors from poor acoustic windows and spectral broadening due to the exponentiation of velocities in the Bernoulli equation. Third, arm-leg pressure difference can only give an indication of the pressure gradient across the stenosis. Finally, catheterization, echocardiography and arm-leg pressure difference do not provide time-resolved three-dimensional information for the entire thoracic aorta.

Investigation of spatial and temporal pressure characteristics might reveal other factors associated with those complications and thus may improve clinical management and risk stratification in the future. Time-resolved three-dimensional, velocity-encoded phase-contrast magnetic resonance imaging (4D flow MRI) provides the opportunity to derive time-resolved three-dimensional pressure difference maps and thus can be used to noninvasively assess spatial and temporal pressure differences in the entire aorta (7). A previous study using 4D flow MRI reported increased peak pressure differences and time to peak pressure differences in patients after aortic coarctation repair indicating the potential of the technique (8). However, a method for standardized visualization of pressure difference maps and description of normal findings in young healthy volunteers has not yet been published to our knowledge.

Purpose of this study was to develop a method for computing and visualizing pressure differences derived from 4D flow MRI and to compare pressure difference maps of patients with unrepaired and repaired aortic coarctation to young healthy volunteers.

## Methods

### *Patients and volunteers*

The local institutional review board approved the study. Written informed consent was obtained. Four patients with aortic coarctation before or after repair (mean age 17 years, age range 3-28, one female, three males) and four young healthy volunteers without history of cardiovascular disease and normal blood pressure (mean age 24 years, age range 20-27, one female, three males) were included. Clinical characteristics of patients and volunteers including operating techniques are listed in *Table 1*.

### *Image acquisition*

A 1.5-T clinical MR scanner (Magnetom Avanto, Siemens, Erlangen, Germany) and one or two standard phased array body coils depending on patient height were used for image acquisition. The standard 4D flow MRI sequence supplied by the manufacturer was applied to both patients and volunteers in an oblique sagittal orientation resulting in a three-dimensional stack of two-dimensional planes with three-directional velocity-encoding (9,10). For patients, the sequence was acquired at the same time of a routinely performed clinical MRI. The following sequence parameters were used: Retrospective ECG gating; FOV, 400 mm × 300 mm; 15-25 adjacent slices as required to cover the entire thoracic aorta; distance factor -30%; slice thickness, 3 mm; in-plane resolution, 1.6 mm × 1.6 mm; reconstructed voxel size, 1.6×1.6×2.1 mm<sup>3</sup>; repetition/echo time (TR/TE), 15.30/4.05 ms; flip angle, 30°; velocity encoding gradient (VENC), 350 cm/s for patients, 150 cm/s for volunteers. The number of calculated phases (time steps) was determined according to the heart rate, with a mean of 25.3±5.2 for patients and 29.6±4.2 for volunteers. The temporal resolution was 28 ms. Acquisition time for 4D flow MRI was 15-20 min depending on heart rate.

### *Segmentation and relative pressure computation*

Image analysis was performed with in-house developed image processing software (10). Phase-offset errors were corrected using a published automated quadratic curve-fitting correction algorithm (11). Subsequently, 4D vessel segmentation was performed based on various flow and morphology features. In principle, an aortic centerline is computed on the basis of vector flow information (12). In the following, the vessel lumen is segmented by applying a

**Table 1** Clinical characteristics of patients and volunteers

	Gender	Age	Hypertension	Type of repair	Result at time of MRI
<b>Patients</b>					
Patient 1	M	3	No	–	No indication for repair
Patient 2	M	11	No	Resection and end-to-end anastomosis	Good result of repair
Patient 3	M	24	No	Resection and patch aortoplasty	Good result of repair with residual narrowing without need for reintervention
Patient 4	F	28	Yes	Resection and end-to-end anastomosis	Good result of repair with residual narrowing without need for reintervention
<b>Volunteers</b>					
Volunteer 1	M	20	No	–	–
Volunteer 2	M	22	No	–	–
Volunteer 3	M	25	No	–	–
Volunteer 4	F	27	No	–	–

feature weighted rating algorithm. After segmentation, the field of flow velocities  $v(x,y,z,t)$  is known throughout vessel volume and heart cycle.

Computation of relative pressure maps from the flow field consists of two major steps (13). In the first step, the field of pressure gradients  $\nabla p$  is computed from the flow velocity field using the momentum conservation

$$\nabla p(x,y,z,t) = -\rho \frac{\partial v(x,y,z,t)}{\partial t} - \rho(v(x,y,z,t) \cdot \nabla)v(x,y,z,t) + \mu \nabla^2 v(x,y,z,t) + \rho g$$

of the Navier-Stokes equation, where  $\rho$  is blood density,  $\mu$  is dynamic viscosity and  $g$  is vector of gravitational force. In this case, blood is modeled as an incompressible, Newtonian fluid and laminar flow without turbulent behavior is assumed. The Navier-Stokes equation is discretized using central differences.

In the second step, a map of relative pressure values is computed from the pressure gradient field by numerical integration. This step is carried out independently for every time step  $t$  in the heart cycle. The term “relative” refers to the fact that the pressures are not given as absolute values, but as differences to one reference point in the vessel volume.

In principle, the relative pressure at an arbitrary point  $(x,y,z)$  in the vessel volume can be computed using a single curve integral between the point  $(x,y,z)$  and the reference point. In theory, the value of the integral is independent from the chosen integration path. However, the quality of the pressure gradient field suffers from image noise of the MRI acquisition. Thus, the value of a curve integral depends on the integration path and a single curve integral

would lead to inaccurate results.

In order to achieve accurate results, the algorithm uses multiple curve integrals with differing integration paths between  $(x,y,z)$  and the reference point to compute the relative pressure at the point  $(x,y,z)$ . The integration paths are automatically defined using a set of traverse lines in an isotropic array of auxiliary points (13). The value of each curve integral is numerically computed and the relative pressure at the point  $(x,y,z)$  is defined as the arithmetic mean of all curve integrals. By applying this approach to every point inside the vessel volume, the software calculates complete maps of relative pressure values.

#### *Standardized visualization of pressure difference maps*

A standardized method for intuitive visualization of pressure difference maps was developed and will be described in the following.

A reference cross-section in the proximal ascending aorta was set as 0 mmHg for all time steps. Color-coded maps were generated with blue color representing lowest relative pressures and red color representing highest relative pressures with a range from  $-20$  to  $+10$  mmHg. For each patient and volunteer, a parasagittal oblique multiplanar reformation of the 4D data set at mid systole was created showing the entire thoracic aorta. To standardize the time step taken for visualization, mid systole was defined as the time step with the maximum flow rate.

For each patient and volunteer, an additional visualization

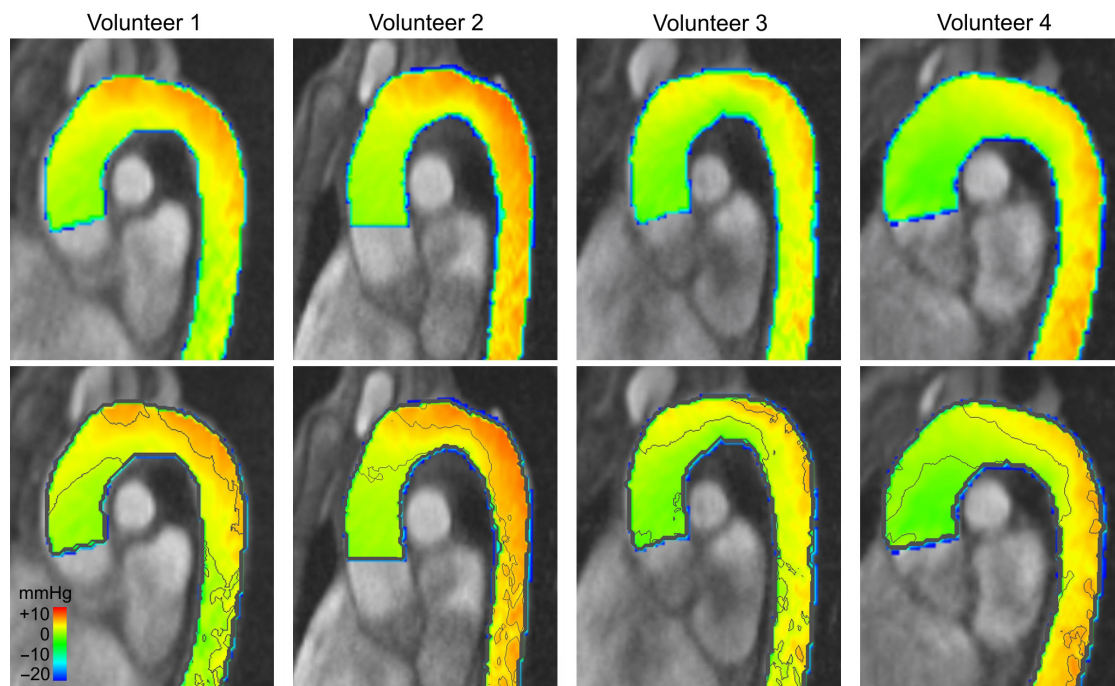


**Figure 1** Color-coded pressure difference maps at mid systole in four young healthy volunteers. Observations are described and discussed in the text. The lower row represents identical views with added isobars (lines connecting points of equal relative pressures) at intervals of 2.5 mmHg.

of the same parasagittal oblique multiplanar reformation was created by adding so-called isobars. Isobars in the present context are lines connecting points of equal relative pressures. Isobars were created at equal pressure intervals of 2.5 mmHg in the displayed pressure range.

## Results

Segmentation, computation of relative pressure maps and visualization of pressure difference maps was successful in all four healthy volunteers and all four patients.

### *Evaluation of healthy volunteers*

All healthy volunteers demonstrated similar pressure difference maps (Figure 1). Pressure difference maps showed smooth and regular distribution of relative pressures in the thoracic aorta at mid systole. Relative pressures of 0-2.5 mmHg were present in the proximal ascending aorta and along the inner curvature up to the proximal aortic arch. Relative pressures increased towards the outer curvature and towards the distal aortic arch with highest relative pressures of 5-7.5 mmHg in the distal aortic arch along the outer curvature. In the descending thoracic aorta, a minor

decrease of relative pressures could be observed without sudden pressure difference drops or peaks.

### *Evaluation of patients*

Pressure difference maps at mid systole of patients demonstrated disturbed pressures compared to volunteers (Figure 2, Video 1) and will be described further in the following. Patient 1, with unrepaired aortic coarctation without indication for repair, and patient 2, with good result of aortic coarctation repair, exhibited similar pressure difference maps. In both patients, relative pressures along the outer curvature of the aortic arch were slightly elevated compared to the inner curvature, but the difference was smaller compared to healthy volunteers. Both patients then showed a local pressure drop of 12 mmHg at the aortic isthmus, with relative pressures regaining the level of the distal aortic arch just distal to the isthmus region. In the following descending thoracic aorta, pressure levels remained constant in these two patients.

Patients 3 and 4, both with good result of repair but with residual narrowing without need for reintervention, demonstrated higher relative pressures in the aortic arch compared to patients 1 and 2. Relative pressures were

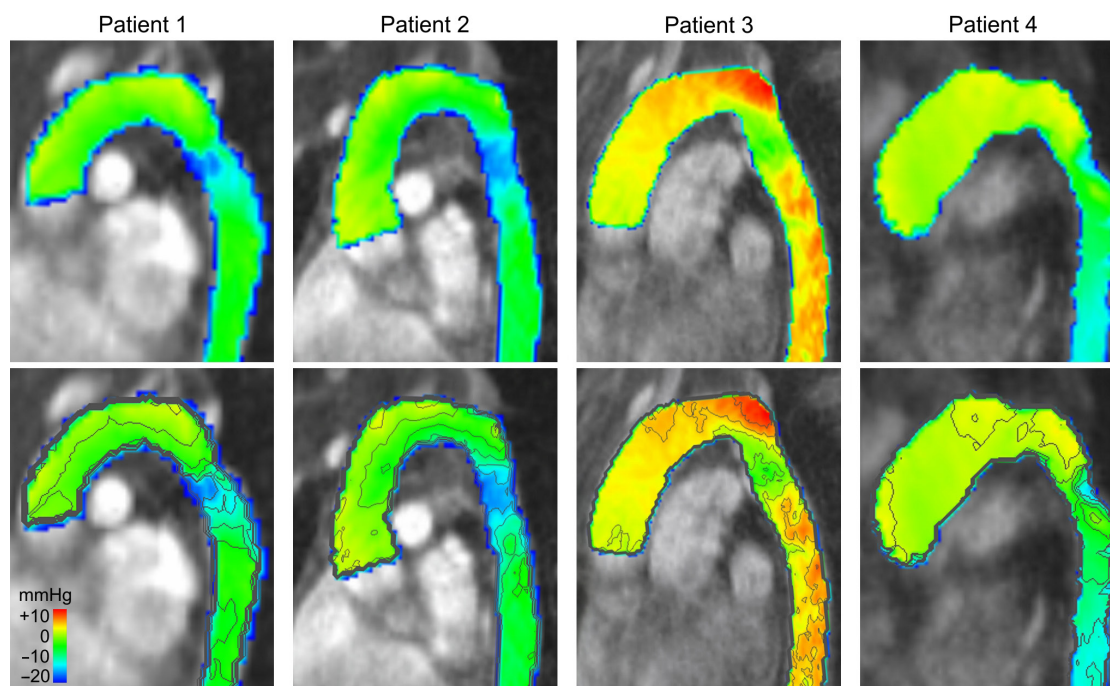


**Figure 2** Color-coded pressure difference maps at mid systole in four patients with aortic coarctation before (patient 1) and after repair (patients 2-4). Observations are described and discussed in the text. The lower row represents identical views with added isobars (lines connecting points of equal relative pressures) at intervals of 2.5 mmHg.



**Video 1** Time-resolved color-coded pressure difference maps of the patient named “patient 2” in *Table 1*, an 11-year-old male patient after resection of aortic coarctation and end-to-end anastomosis. Observations are described and discussed in the text.

particularly high in patient 3 reaching +10 mmHg, the only patient after patch aortoplasty. Similar to patients 1 and 2, patients 3 and 4 also exhibited a pressure drop at the aortic isthmus, with relative pressures again regaining the level of the distal aortic arch just distal to the isthmus region. In

patient 3, pressure levels remained fairly constant in the following descending thoracic aorta as in patients 1 and 2. In contrast, a considerable continuous pressure decrease could be observed in patient 4, the only patient with hypertension.

## Discussion

Our study presented a new methodology to compute and visualize pressure difference maps based on 4D flow MRI data in a standardized way. The methodology was successfully applied to healthy volunteers and four patients with aortic coarctation, with three patients after coarctation repair. Young healthy volunteers exhibited smooth and regular distribution of relative pressures in the thoracic aorta at mid systole with very similar distribution in all analyzed volunteers. In contrast, patients demonstrated abnormal features of pressure differences. Most notably, all patients showed some degree of pressure drop at the aortic isthmus, including patient 2 with good result after resection of aortic coarctation and end-to-end anastomosis. Further changes of pressure difference maps could be detected and will be discussed in the following.

Our study demonstrated pressure drops at the aortic

isthmus in all patients. The pressure drop in patient 2 with good result after repair is in accordance with previous studies showing that there frequently is a residual pressure gradient even after successful resection of aortic coarctation (14,15). The pressure drops visualized in the present study can also be quantified based on 4D flow MRI data as published in a previous study (16). The combination of visualization and quantification of pressure drops at the aortic isthmus may be an intuitive and accurate method to determine presence and location of hemodynamically relevant narrowings.

Another interesting finding of our study was the increased relative pressures in the aortic arch, i.e., proximal to the aortic isthmus, in patients 3 and 4 with residual narrowing at the aortic isthmus after repair, as opposed to patient 2 with good result after repair. This is in accordance with the physical relationship between the degree of a vascular stenosis and the pressure proximal to the stenosis at peak forward flow. In short, the irregular vessel shape accompanying a relevant stenosis can lead to a significant blood deceleration proximal to the narrowing. In this case, the kinetic energy is partially transformed into static pressure energy. Differentiation between hemodynamically relevant residual narrowing and good result after repair may be of prognostic significance as indicated by a previous study (17). Therefore, further investigation and quantification of the observation in our study is desirable in a larger patient cohort.

Finally, we observed increased relative pressures both in the aortic arch and the descending aorta in patient 3 with residual narrowing after resection and patch aortoplasty. Increased relative pressures particularly in the descending aorta might play a role in the formation of aneurysms, a complication that occurs more frequently in patients with aortic coarctation after patch aortoplasty compared to end-to-end anastomosis (18-20). It has to be noted that the finding might also occur in patients with other operating techniques. Further studies are required to investigate the significance of the finding. A potential explanation for increased relative pressures might be altered vascular resistance. In the aortic arch, the increased relative pressure might be at least partially explained by the residual narrowing as discussed above.

To our knowledge, this is the first study to present a method for standardized visualization of pressure difference maps and describe normal findings of pressure difference maps in young healthy volunteers. In addition to visualization, the technique can be used to quantify pressure gradients potentially allowing for noninvasive

pressure gradient measurements correlating to invasive measurements in the future (21). This gives the perspective that the technique will enable assessment of hemodynamic significance of aortic coarctation which is currently done by invasive catheterization or exercise- or drug-induced stress tests.

The major limitation of the present study is the limited number of patients. However, the focus of the present study was to develop and present a technique for computation and visualization of pressure difference maps derived from 4D flow MRI that can be applied to larger cohorts. Given the small number of patients, the observations cannot be generalized. However, they indicate that there are relevant alterations of spatial pressure distribution in patients with repaired and unrepaired aortic coarctation that are worth to be investigated further. Another limitation is that the present study did not include a validation against gold standard invasive catheterization. None of the included patients had an indication for catheterization at the time of the MRI though. Prior to begin of the present study, we performed extensive phantom experiments validating the pressure calculations derived from 4D flow MRI against invasive catheter measurements. These experiments showed good agreement of calculated pressure differences with invasively measured pressures (21).

In conclusion, pressure difference maps derived from 4D flow MRI can depict alterations of spatial pressure distribution in patients with repaired and unrepaired aortic coarctation. The technique might allow identifying pathophysiological conditions underlying complications after aortic coarctation repair and thus help to guide imaging surveillance intervals as well as medical and surgical therapy in the future. Studies involving more patients are warranted to systematically investigate alterations depicted by the present study.

## Acknowledgements

This work was supported by the German Research Foundation (DFG) within the “Research training group 1126: Intelligent Surgery—Development of new computer-based methods for the future workplace in surgery”. Michael Delles received support within DFG Grant UN 306/1-1.

*Disclosure:* The authors declare no conflict of interest.

## References

1. Tronc F, Curtil A, Robin J, et al. Coarctation of the

- aorta and its surgical treatment. *Arch Mal Coeur Vaiss* 1997;90:1729-36.
2. Hamdan MA, Maheshwari S, Fahey JT, et al. Endovascular stents for coarctation of the aorta: initial results and intermediate-term follow-up. *J Am Coll Cardiol* 2001;38:1518-23.
  3. Oliver JM, Gallego P, Gonzalez A, et al. Risk factors for aortic complications in adults with coarctation of the aorta. *J Am Coll Cardiol* 2004;44:1641-7.
  4. Bogaert J, Gewillig M, Rademakers F, et al. Transverse arch hypoplasia predisposes to aneurysm formation at the repair site after patch angioplasty for coarctation of the aorta. *J Am Coll Cardiol* 1995;26:521-7.
  5. Kappetein AP, Zwinderman AH, Bogers AJ, et al. More than thirty-five years of coarctation repair. An unexpected high relapse rate. *J Thorac Cardiovasc Surg* 1994;107:87-95.
  6. de Divitiis M, Pilla C, Kattenhorn M, et al. Vascular dysfunction after repair of coarctation of the aorta: impact of early surgery. *Circulation* 2001;104:II165-70.
  7. Tyszka JM, Laidlaw DH, Asa JW, et al. Three-dimensional, time-resolved (4D) relative pressure mapping using magnetic resonance imaging. *J Magn Reson Imaging* 2000;12:321-9.
  8. Bock J, Frydrychowicz A, Lorenz R, et al. In vivo noninvasive 4D pressure difference mapping in the human aorta: phantom comparison and application in healthy volunteers and patients. *Magn Reson Med* 2011;66:1079-88.
  9. Bogren HG, Buonocore MH. 4D magnetic resonance velocity mapping of blood flow patterns in the aorta in young vs. elderly normal subjects. *J Magn Reson Imaging* 1999;10:861-9.
  10. Unterhinninghofen R, Ley S, Ley-Zaporozhan J, et al. Concepts for visualization of multidirectional phase-contrast MRI of the heart and large thoracic vessels. *Acad Radiol* 2008;15:361-9.
  11. Delles M, Rengier F, von Tengg-Kobligk H, et al. Quadratic phase offset error correction of velocity-encoded magnetic resonance imaging data. *Int J Comput Assist Radiol Surg* 2009;4 Suppl 1:10-1.
  12. Jeong YJ, Ley S, Dillmann R, et al. Vessel centerline extraction in phase-contrast MR images using vector flow information. *Proc SPIE* 2012;8314:83143H.
  13. Delles M, Unterhinninghofen R, Ley S, et al. Integration of relative blood pressure fields from magnetic resonance-based pressure gradient measurements. *Int J Comput Assist Radiol Surg* 2010;5 Suppl 1:89-90.
  14. Ong CM, Canter CE, Gutierrez FR, et al. Increased stiffness and persistent narrowing of the aorta after successful repair of coarctation of the aorta: relationship to left ventricular mass and blood pressure at rest and with exercise. *Am Heart J* 1992;123:1594-600.
  15. Rodés-Cabau J, Miró J, Dancea A, et al. Comparison of surgical and transcatheter treatment for native coarctation of the aorta in patients > or = 1 year old. The Quebec Native Coarctation of the Aorta study. *Am Heart J* 2007;154:186-92.
  16. Bock J, Frydrychowicz A, Lorenz R, et al. In vivo noninvasive 4D pressure difference mapping in the human aorta: phantom comparison and application in healthy volunteers and patients. *Magn Reson Med* 2011;66:1079-88.
  17. Vriend JW, Zwinderman AH, de Groot E, et al. Predictive value of mild, residual descending aortic narrowing for blood pressure and vascular damage in patients after repair of aortic coarctation. *Eur Heart J* 2005;26:84-90.
  18. Cramer JW, Ginde S, Bartz PJ, et al. Aortic aneurysms remain a significant source of morbidity and mortality after use of Dacron(®) patch aortoplasty to repair coarctation of the aorta: results from a single center. *Pediatr Cardiol* 2013;34:296-301.
  19. Clarkson PM, Nicholson MR, Barratt-Boyes BG, et al. Results after repair of coarctation of the aorta beyond infancy: a 10 to 28 year follow-up with particular reference to late systemic hypertension. *Am J Cardiol* 1983;51:1481-8.
  20. Presbitero P, Demarie D, Villani M, et al. Long term results (15-30 years) of surgical repair of aortic coarctation. *Br Heart J* 1987;57:462-7.
  21. Delles M, Rengier F, Ley S, et al. Influence of imaging quality on magnetic resonance-based pressure gradient measurements. *Proc SPIE* 2010;7626:762624.

**Cite this article as:** Rengier F, Delles M, Eichhorn J, Azad YJ, von Tengg-Kobligk H, Ley-Zaporozhan J, Dillmann R, Kauczor HU, Unterhinninghofen R, Ley S. Noninvasive pressure difference mapping derived from 4D flow MRI in patients with unrepaired and repaired aortic coarctation. *Cardiovasc Diagn Ther* 2014;4(2):97-103. doi: 10.3978/j.issn.2223-3652.2014.03.03